



# POD analysis of photospheric velocity field: solar oscillations and granulation

A. Vecchio<sup>1</sup>, V. Carbone<sup>1</sup>, F. Lepreti<sup>1</sup>, L. Primavera<sup>1</sup>, P. Veltri<sup>1</sup>, L. Sorriso-Valvo<sup>2</sup>,  
Th. Straus<sup>3</sup>

<sup>1</sup> Dipartimento di Fisica, Università della Calabria, and Istituto Nazionale di Fisica della Materia, Unità di Cosenza, 87030 Rende (CS), Italy

<sup>2</sup> Liquid Crystal Laboratory - INFN/CNR - 87036 Rende (CS), Italy

<sup>3</sup> INAF - Osservatorio Astronomico di Capodimonte, Napoli, Italy  
e-mail: vecchio@fis.unical.it

**Abstract.** The spatio-temporal dynamics of the solar photosphere is studied by performing a Proper Orthogonal Decomposition (POD) of line of sight velocity fields computed from high resolution data coming from the MDI/SOHO instrument. Using this technique, we are able to identify and characterize the different dynamical regimes acting in the system. Low frequency oscillations, with frequencies in the range 20–130  $\mu\text{Hz}$ , dominate the most energetic POD modes (excluding solar rotation), and are characterized by spatial patterns with typical scales of about 3 Mm. Patterns with larger typical scales of  $\approx 10$  Mm, are associated to p-modes oscillations at frequencies of about 3000  $\mu\text{Hz}$ .

**Key words.** Sun, solar oscillations, convective turbulence

## 1. Introduction

The solar photosphere is an interesting example of a system exhibiting complex spatio-temporal behavior. The early research in pattern formation focused on the presence of simple periodic structures, while the main questions currently addressed concern regimes characterized by higher complexity, that is, patterns that are more irregular in space and time. This is often related to the occurrence of intermediate states between order and turbulence (Akhromeyeva et al. 1989). Indeed on the solar surface the turbulent evolution of granulation coexist with the contribution of solar global oscillations with peculiar discrete fre-

quencies (Leighton et al. 1962; Severnyet al. 1976; Brookes et al. 1978; Thomson et al. 1995; Cristensen-Dalgaard 2002). Two main modes can be excited, namely acoustic p-modes, the 5 minutes oscillations, (in the range 1000–5000  $\mu\text{Hz}$  (Ulrich 1970)) and gravitational g-modes (in the range 1–200  $\mu\text{Hz}$ ). The Fourier analysis of spatio-temporal maps of LOS velocity fields on the solar photosphere, the so-called  $k$ - $\omega$  spectra, shows ridges corresponding to the discrete p-modes (Deubner 1974, 1975)(see fig.1). On the other hand, discrete frequencies in the low-frequency (g-modes) range are not recognized, but rather the power observed in this range is spread over a continuum, commonly attributed to the solar turbulent convection (Harvey 1985).

*Send offprint requests to:* A. Vecchio

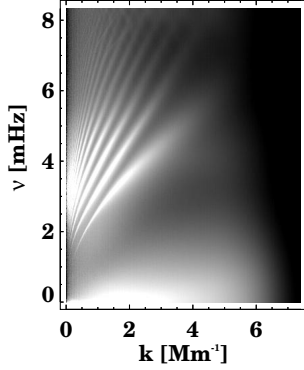


**Fig. 1.** The  $k$ - $\omega$  spectrum of the dataset.

## 2. The POD technique

In the present paper, we use the Proper Orthogonal Decomposition (POD) as a powerful tool to investigate the dynamics of stochastic spatio-temporal fields. In astrophysical contexts, POD has been recently used to analyze the spatio-temporal dynamics of the solar cycle (Mininni et al. 2002). Introduced in the context of turbulence (Holmes et al. 1996), the POD decomposes a field  $u(\mathbf{r}, t)$  as  $u(\mathbf{r}, t) = \sum_{j=0}^{\infty} a_j(t) \Psi_j(\mathbf{r})$  (1), the eigenfunctions  $\Psi_j$  being constructed by maximizing the average projection of the field onto  $\Psi_j$ , constrained to the unitary norm. Averaging leads to an optimization problem that can be cast as  $\int_{\Omega} \langle u(\mathbf{r}, \mathbf{t}), u(\mathbf{r}', \mathbf{t}) \rangle \Psi(\mathbf{r}') d\mathbf{r}' = \lambda \Psi(\mathbf{r})$  (2), where  $\Omega$  represents the spatial domain and brackets represent time averages. The integral equation (2) provides the eigenfunctions  $\Psi_j$  and a countable, infinite set of ordered eigenvalues  $\lambda_j \geq \lambda_{j+1}$ , each representing the kinetic energy of the  $j$ -th mode. Thus, POD builds up the basis functions, which are not given *a priori*, but rather obtained from observations. The time coefficients  $a_j(t)$  are then computed from the projection of the data on the corresponding basis functions  $\Psi_j(\mathbf{r})$  so that the sum (1), when truncated to  $N$  terms, contains the largest possible energy with respect to any other linear decomposition of the same truncation order. This method is particularly appropriate when analyzing complex physical systems, where differ-

ent dynamical regimes coexist. POD allows to identify these regimes and to characterize their energetics and their spatial structure.

## 3. Data analysis

The POD has been applied to the time evolution line of sight velocity field  $u(x, y, t)$  ( $x, y$  being the coordinates on the surface of the Sun), obtained from MDI mounted on SOHO. The field of view is  $695 \times 695$  pixels, with a spatial resolution of about 0.6 arcsec. Total time lasts about 15 hours and images are acquired every minute, so that we have  $N = 886$  images. In this way we get a set of eigenfunctions  $\psi_j(x, y)$  and coefficients  $a_j(t)$ , as well as the sequence of eigenvalues  $\lambda_j$  ( $j = 0, 1, \dots, N$ ). Most of the energy is associated with the first POD mode, accounting for the line of sight component of solar rotation. As this is not related to turbulence or solar oscillations, this mode will be ignored throughout this paper. The rest of the energy is decreasingly shared by the following 885 modes, so that, for example, only 4% is associated to the second ( $j = 1$ ) POD mode. In laboratory turbulent flows, POD attribute almost 90% of total energy to the typical large-scale coherent structures, confined to  $j \leq 2$  (Alfonsi and Primavera 2002). In our case, 90% of energy (excluding the rotation) is contained in the first 140 modes. This indicates the absence of dominating large-scale structures and the presence of some turbulent dynamics related to nonlinear interactions among different modes and structures at all scales. For each value of  $j$  two well defined frequencies are clearly observed: the first one in the low frequency range and the second one in the range where p-modes are usually observed. As an example in fig. (2) we report the time evolution of coefficients  $a_j(t)$  and the corresponding frequency spectra  $|a_j(\nu)|^2$ , obtained through temporal Fourier transform for three values of  $j$ . Concerning the spatial pattern, each value of the mode  $j$  is associated to a wide range of wave vectors. This can be seen in fig. (3) where we show the eigenfunctions  $\psi_j(x, y)$  and the corresponding wave vector spectra  $|\psi_j(k)|^2$  (where  $k^2 = k_x^2 + k_y^2$ ), obtained through spatial Fourier transform of

$\psi_j(x, y)$ . Thus, modes can be separated in three different groups, accordingly to grain size, and temporal behaviour. The  $1 \leq j \leq 11$ , most energetic modes display a pattern with very fine structures, recalling the photospheric granulation, with a broad spectrum, and clearly show a center-limb modulation. This kind of eigenfunctions are associated with time coefficients dominated by low-frequency oscillations in the range 20–127  $\mu\text{Hz}$ . Conversely, eigenfunctions of the modes  $j = 12$  and  $j = 13$  present a coarser pattern, and their (still broad) spectra show ridges. In this case high frequency oscillations, in the range 3250–3550  $\mu\text{Hz}$ , prevail. The further lower energy modes cannot be precisely classified, and seem to present a mixture of the previous characteristics, both in grain size and in spectral shape. The amplitudes of the two peaks, in time power spectrum, are found to be of the same order. The spatial pattern associated to each mode, although complicated, can be quantitatively characterized by computing the integral scale length  $L_j = \int_0^\infty |\psi_j(k)|^2 k^{-1} dk / \int_0^\infty |\psi_j(k)|^2 dk$  which represents the energy containing scale of classical turbulence (Pope 2000). This allows to estimate the typical scale for the first ten fine grained modes  $L \simeq 3$  Mm, while for the coarse grained modes  $L \simeq 10$  Mm. Let us first focus on the high-frequency modes. Both the informations on the involved spatial scales and the measured frequencies indicate that solar p-mode contributions are identified by POD. Indeed, the frequencies we observe have been predicted by helioseismological models cf. Cristensen-Dalsgaard (2002), and are well known from observations using Fourier techniques (Deubner 1975; Leibacher et al. 2000). The spatial pattern of about 10 Mm, which POD associates with high frequency modes, is in agreement with the horizontal coherence length attributed to solar p-modes. In order to confirm this, we compared the  $k$ – $\omega$  classical results with the POD spectra. Choosing, for example, the POD mode  $j = 12$ , we performed a cut of the  $k$ – $\omega$  spectrum at the measured peak frequency (3254  $\mu\text{Hz}$ ). We thus obtain a wavelength spectrum, reported on figure3, that can be compared with the  $j = 12$  eigenfunction spectrum. As can be seen, the spikes ob-

served in the POD spectrum qualitatively correspond to the typical ridges structure of the  $k$ – $\omega$  spectrum. Concerning the low-frequency dominated modes, it is interesting to note that the measured frequency range, mentioned above, is compatible with the theoretical results on solar gravitational modes (Cristensen-Dalsgaard 2002). However, because of the resolution limit, related to the finite length of the time series, the low frequency oscillations detected by POD can not be unambiguously attributed to discrete modes, rather than to a continuum. The evidence of center-limb modulation shows that such modes are mainly associated with the contribution of horizontal velocities.

#### 4. Conclusions

We presented the first application of POD on high resolution solar photospheric velocity fields, which represents an example of convec-

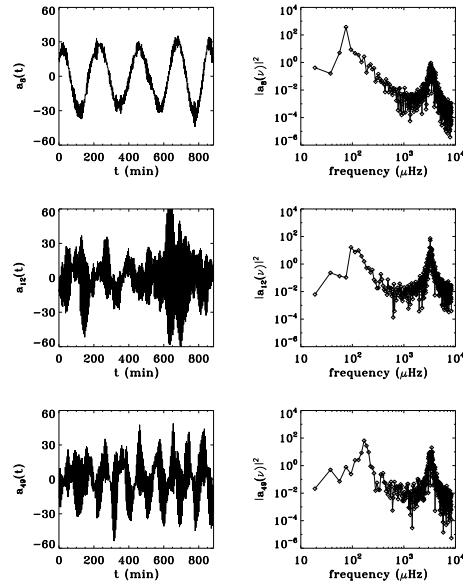


**Fig. 2.** In the left-hand column we report the time evolution of POD coefficients  $a_j(t)$  (m/s) for the modes  $j = 8, 12, 49$ . In the right-hand column we report the corresponding frequency spectra  $|a_j(\nu)|^2$  ( $\text{m}^2/\text{s}^2$ ).

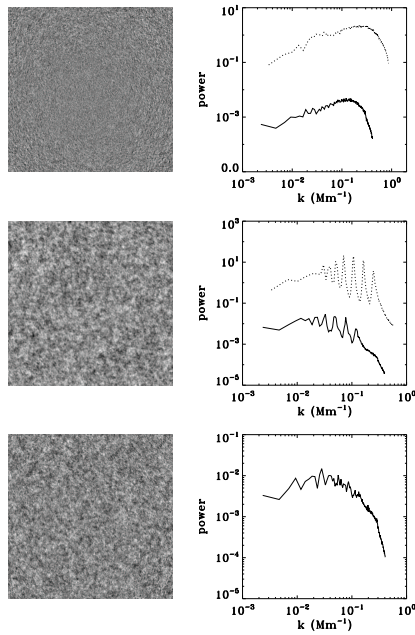


**Fig. 3.** In the left-hand column we report from top to bottom the POD eigenfunctions  $\Psi_j(x, y)$  for three the modes  $j = 8$ ,  $j = 12$  and  $j = 49$ . In the right hand column we report the wave vector spectra  $|\Psi_j(k)|^2$  of the corresponding images. Superimposed on the second and third spectra, the wave vector spectra obtained from the  $k$ - $\omega$  cut, respectively at  $\omega = 3254 \mu\text{Hz}$  and  $\omega = 76 \mu\text{Hz}$ , are represented (dotted lines, in arbitrary units).

tive turbulence in high Rayleigh numbers natural fluids. POD is able to capture the main energetic and spatial features of the solar photosphere. Two main oscillatory processes, well separated in frequency, are detected in the range  $3250$ – $3550 \mu\text{Hz}$  and in the range  $20$ – $130 \mu\text{Hz}$ . The high frequency waves are the well known acoustic p-modes and their properties, as obtained from POD, are in agreement with previous results based on Fourier techniques. On the other hand, low frequency oscillations, with frequencies compatible with those expected from the theory of solar g-modes, prevail in the most energetic POD modes (excluding solar rotation), which are characterized

by spatial eigenfunctions with typical scales of  $\approx 3 \text{ Mm}$ . The clear association between low frequency oscillations and small spatial scales, which are close to the solar granulation, is the most interesting result provided by our analysis. This suggests the presence of strong coupling between low frequency modes and the turbulent convection. As a consequence, the use of empirical eigenfunctions for the description of such system seems appropriate, and a further improvement of this analysis can be expected from its application to longer time series.

## References

- Akhromeyeva, T. S., et al. 1989, Phys. Rep. 176, 189
- Alfonsi, G. and Primavera, L. 2002, J. of Flow visualization and Image Processing 9, 89
- Brookes, J. R., Isaak, G. R., Von der Raay, H. B. 1978, Nature 259, 92
- Cristensen-Dalsgaard 2002, J., Rev. Mod. Phys. 74, 1073
- Deubner, F.-L. 1974, A&A 39, 31
- Deubner, F.-L. 1975, A&A 44, 371
- Harvey, J. 1985, in Future missions in solar heliospheric and space plasma physics ESA SP-235, Noordwijk, 199
- Holmes, P., Lumley, J., Berkooz, L. G. 1996, Turbulence, Coherent Structures, Dynamical Systems and Symmetry, Cambridge Univ. Press
- Leibacher, J. W., Noyes, R. W., Toomre, J., Ulrich, R. K. 2000, Scient. Amer. 253, No. 3, 34
- Leighton, R. B., Noyes, R. W., Simon, G. W. 1962, ApJ 135, 474
- Mininni, P. D., Gómez, D. O., Mindlin, G. B. 2002, Phys. Rev. Lett. 89, 061101
- Pope, S. B. 2000, Turbulent flows, Cambridge Univ. Press
- Severny, A. B., Kotov, V. A. 1976, Tsap, T. T., Nature 259, 87
- Thomson, D. J., MacLennan, C. G., Lanzerotti, L. J. 1995, Nature 376, 139
- Ulrich, R. K. 1970, ApJ 162, 993